Labeling and Evaluation of *N*-[^{11}C]Methylated Quinoline-2-carboxamides as Potential Radioligands for Visualization of Peripheral Benzodiazepine Receptors

Mario Matarrese,[†] Rosa Maria Moresco,[†] Andrea Cappelli,[‡] Maurizio Anzini,[§] Salvatore Vomero,[‡] Pasquale Simonelli,[†] Elisa Verza,[†] Fulvio Magni,[†] Francesco Sudati,[†] Dmitri Soloviev,[†] Sergio Todde,[†] Assunta Carpinelli,[†] Marzia Galli Kienle,*[,†] and Ferruccio Fazio[†]

INB-CNR, University of Milano/Bicocca, Institute H.S. Raffaele, Via Olgettina 60, 20132 Milano, Italy, Dipartimento Farmaco Chimico Tecnologico, Università di Siena, Via Aldo Moro, 53100 Siena, Italy, and Dipartimento di Scienze Farmacobiologiche, Università di Catanzaro "Magna Graecia", Complesso "Ninì Barbieri", 88021 Roccelletta di Borgia (CZ), Italy

Received June 6, 2000

The novel quinoline-2-carboxamide derivatives *N*-[*methyl*-^{11}C]-3-methyl-4-phenyl-*N*-(phenylmethyl)quinoline-2-carboxamide ([^{11}C]**4**), (±)-*N*-[*methyl*-^{11}C]-3-methyl-*N*-(1-methylpropyl)-4-phenylquinoline-2-carboxamide ([^{11}C]**5**), and (±)-*N*-[*methyl*-^{11}C]-3-methyl-4-(2-fluorophenyl)-*N*-(1-methylpropyl)quinoline-2-carboxamide ([^{11}C]**6**) were labeled with carbon-11 ($t_{1/2}$ = 20.4 min, β^+ = 99.8%) as potential radioligands for the noninvasive assessment of peripheral benzodiazepine type receptors (PBR) in vivo with positron emission tomography (PET). The radiosynthesis consisted of *N*-methylation of the desmethyl precursors 3-methyl-4-phenyl-*N*-(phenylmethyl)quinoline-2-carboxamide (**4a**), (±)-3-methyl-*N*-(1-methylpropyl)-4-phenylquinoline-2-carboxamide (**5a**), and (±)-4-(2-fluorophenyl)-3-methyl-*N*-(1-methylpropyl)quinoline-2-carboxamide (**6a**) with either [^{11}C]methyl iodide or [^{11}C]methyl triflate in the presence of tetrabutylammonium hydroxide or potassium hydroxide in dimethylformamide. The radioligands [^{11}C]**4**, [^{11}C]**5**, and [^{11}C]**6** were synthesized with over 99% radiochemical purity in 30 min, 30 ± 5% radiochemical yield, calculated at the end of synthesis (EOS) non-decay-corrected, and 2.5 ± 1.2 Ci/μmol of specific radioactivity. Inhibition studies in rats following intravenous pre-administration of 1-(2-chlorophenyl)-*N*-methyl-*N*-(1-methylpropyl)-3-isoquinolinecarboxamide (PK 11195, **1**) showed high specific binding to PBR of [^{11}C]**4**, [^{11}C]**5**, and [^{11}C]**6** in heart, lung, kidney, adrenal gland, spleen, and brain. The biological data suggest that [^{11}C]**5**, [^{11}C]**6**, and particularly [^{11}C]**4** are promising radioligands for PBR imaging in vivo with PET.

Introduction

The presence of two distinct benzodiazepine binding sites, the central and peripheral benzodiazepine receptors, has been described in mammalian tissue.[1,2] The central benzodiazepine receptor (CBR) is expressed in the central nervous system and is part of the $GABA_A$ receptor macromolecular complex which includes a binding site for the inhibitory neurotransmitter γ-aminobutyric acid (GABA) and a chloride ion channel.[13] The peripheral-type benzodiazepine binding site (PBR), also known as the ω_3 binding site,[4] is anatomically and pharmacologically distinct from the CBRs.[5,6] PBRs are mainly localized in peripheral tissues and glial cells. They are highly expressed in steroidogenic tissues such as adrenal gland[7] but also in kidney,[1,8] heart,[9] testis,[8] and at a lower level in the brain parenchyma, ependyma, choroid plexus, and olfactory neurons.[10]

The function of PBRs is still unknown, but their localization on the outer membrane of the mitochondria[11] suggests a role in the modulation of mitochondrial function and the immune system. Moreover, their involvement in cell proliferation, steroidogenesis, calcium flow, cellular respiration, and malignancy has been considered (see ref 6 for an extensive review on the pharmacology and clinical implication of PBR). Preclinical studies on animal models of brain injuries support the idea of the use of PBR as a marker of brain gliosis associated with neuronal cell death[12,13] which could be used as an early indicator of the neurodegenerative processes.

Emission tomography techniques and in particular positron emission tomography (PET) enable the in vivo study of several physiological and neurochemical variables in living subjects using methods originally developed for quantitative autoradiography. Thus, interest in the PBR's study with PET has evolved from the observation that an increased concentration of PBR was observed in lesioned brain areas in a variety of neuropathologies such as multiple sclerosis, Alzheimer's disease, and Huntington's disease.[12−16]

1-(2-Chlorophenyl-*N*-methyl-*N*-(1-methylpropyl)-3-isoquinolinecarboxamide (PK 11195, **1**) (Chart 1) labeled with the positron emitter carbon-11[17,18] ($t_{1/2}$ = 20.4 min, β^+ = 99.8%) binds to PBRs, being potentially useful for PBR in imaging of multiple sclerosis,[13,14] brain tumors,[19,20] cerebral infarct,[21] and abnormalities of calcium channel in heart diseases.[22] Compound **1** has high affinity for PBR (IC_{50} = 2.2 nM, K_d = 1.4 nM),[23,24] and its (*R*)-isomer labeled with carbon-11[25] is, so far, the only

* To whom correspondence should be addressed: c/o DIBIT, S. Raffaele, Via Olgettina 58, 20132 Milano, Italy. Tel: 39-02-26434924. Fax: 39-02-26434923. E-mail: marzia.gallikienle@unimib.it.
[†] University of Milano/Bicocca.
[‡] Università di Siena.
[§] Università di Catanzaro "Magna Graecia".

10.1021/jm001004h CCC: $20.00
Published on Web 01/16/2001

Chart 1. Peripheral-Type Benzodiazepine Radioligands

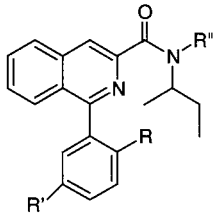

PK 11195, **1** (R=Cl; R'=H; R"=$^{11}CH_3$)
2-Iodo-PK 11195, **2** (R=^{123}I; R'=H; R"=CH_3)
PK 14105, 3 (R=^{18}F; R'=NO_2; R"=CH_3)

PBR radioligand used successfully in PET,[26] although other analogues of PK 11195 labeled with fluorine-18 ($t_{1/2}$ = 109.6 min, β^+ = 97%) such as *N*-methyl-*N*-(1-methylpropyl)-1-(2-fluoro-5-nitrophenyl)isoquinoline-3-carboxamide ([^{18}F]PK 14105,[23] **2**: K_D = 4.8 nM[27]) or with the single-photon emitter iodine-123 ($t_{1/2}$ = 13.2 h) such as 1-(2-iodophenyl)-*N*-methyl-*N*-(1-methylpropyl)isoquonoline-3-carboxamide ([^{123}I]PK 11195,[28] **3**: $K_D \approx 10$ nM)[29] have been synthesized (Chart 1). However, the high lipophilicity (log P = 3.4) and the low bioavailability (88% of tracer bound to plasma proteins)[26,30] might reduce its sensitivity in the in vivo evaluation of PBR using PET. These features of **1** may explain its failure in demonstrating in vivo variations of PBR density associated with microgliosis in Alzheimer's disease.[31] Notwithstanding, [^{11}C]**1** is still the current reference radioligand for the in vivo assessment of PBR in PET studies, while [^{18}F]**3** has not been studied in humans, and the rapid metabolism in the blood of [^{123}I]-**2** (ca. 55% distributed in two polar metabolites)[32] could limit the clinical application of this radioligand.

Recently, the synthesis of new conformationally restrained quinolinecarboxamide analogues of **1**, which could be of potential interest for the in vivo imaging of PBR, has been published.[24] Among the most potent representatives of this class of PBR ligands, compounds **4** (IC_{50} = 2.1 nM), **5** (IC_{50} = 2.1 nM), and **6** (IC_{50} = 2.9 nM) (Chart 2) showed in vitro biological properties, which could be of potential interest for the in vivo imaging of PBR; thus they were chosen as possible candidates for PET radioligands.

In this report we describe ^{11}C radiolabeling of **4**−**6** starting from the corresponding desmethyl precursors **4a**, **5a**, and **6a** and the results of biodistribution and inhibition studies performed in rats to evaluate their potential use as PET radioligands.

Results

Chemistry. Optimization of the radiolabeling conditions was initially carried out using precursor **4a**. Reaction conditions such as solvent base and temperature were varied in the attempt to increase the radiochemical yield (Table 1). The use of [^{11}C]methyl triflate as [^{11}C]methylating agent at temperatures ranging from 10 to 50 °C led to low radiochemical yields (9−40% of [^{11}C]methyl incorporated into the precursor) due to the high hydrolysis rate of the triflate leading to the formation of [^{11}C]methanol (40−75%). Lowering the temperature to −15 °C increased the labeling efficiency, the incorporation of [^{11}C]methyl from [^{11}C]methyl triflate being 60% with a reduced formation of [^{11}C]-

Chart 2. New Quinoline-2-carboxamides

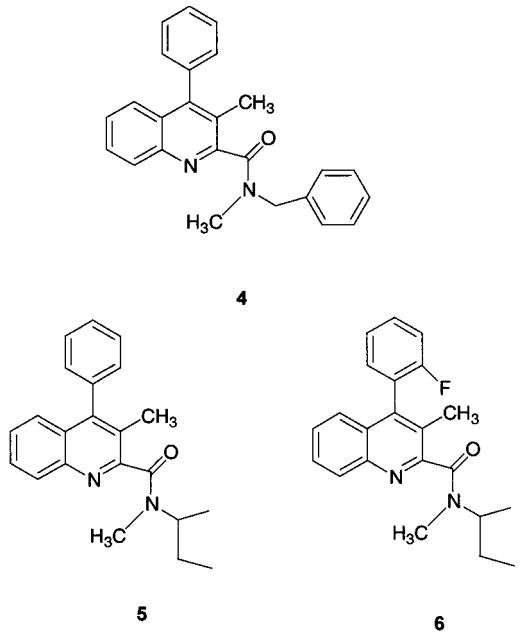

4 **5** **6**

methanol (34%). The reduction of the amount of potassium hydroxide from 10 to 2 μmol in dimethylformamide as reaction solvent at −15 °C caused an increased production of [^{11}C]methanol, which represented 76% of the radioactivity, while the amount of the target compound was reduced approximately to 7%. Dimethylformamide was found to be the solvent of choice for the radiomethylation. Changing the solvent and the base did not give satisfactory results as shown in Table 1.

Better results with **4a** were obtained using [^{11}C]-methyl iodide as the methylating agent at 80 °C in dimethylformamide particularly when potassium hydroxide was substituted by TBAH. The last conditions with **4a** as the precursor gave 84% of the radioactivity associated with the target [^{11}C]methylated compound. Under the same conditions, 84% of radioactivity associated with the target compound was also obtained using **5a** and **6a** as the precursor (Table 1).

The overall non-decay-corrected radiochemical yield of the [^{11}C]*N*-methylation was 30−35% for all radiotracers. The specific radioactivity was 2.5 ± 1.2 Ci/μmol when calculated at the end of the synthesis (EOS) with an average time of radiosynthesis of 30 min, including radioligand formulation for intravenous administration. In the typical experiment starting from 400 mCi of [^{11}C]-CO_2, 100 mCi of the formulated radioligands was obtained with a chemical and radiochemical purity of 99% and 100%, respectively.

Identity of the final radioactive radioligands was confirmed by co-injection with the authentic sample of **4**−**6** on reverse-phase high-pressure liquid chromatography (HPLC) and by the mass spectrometric analysis of the products of the carrier-added radiosyntheses (see Experimental Section). The atmospheric pressure chemical ionization (APCI) mass spectra of [^{11}C]**4** displayed an intense ion at *m*/*z* 367 corresponding to the protonated molecular ion (MH^+). [^{11}C]**4** radioligand was confirmed also by electron impact (EI) mass spectroscopy. The EI spectrum showing a base ion at *m*/*z* 91 ($PhCH_2$) and ions at *m*/*z* 366 (M^+), 275 (M − $PHCH_2$), 246 (M − PhC_2H_5N), and 218 (M − PhC_3H_5NO).

Table 1. Radiolabeling of [^{11}C]**4**, [^{11}C]**5**, and [^{11}C]**6** with [^{11}C]Methyl Iodide and [^{11}C]Methyl Triflate[a]

[^{11}C]synthon	precursor	base	amount (μmol)	temp (°C)	solvent	[^{11}C]radioligands (%)	[^{11}C]CH_3OH (%)	other [^{11}C]impurities (%)	*n*
MeOTf	**4a**	KOH	10	10	HMPA	9	76	14	3
MeOTf	**4a**	KOH	10	25	DMF	43	39	2	3
MeOTf	**4a**	KOH	10	50	DMF	37	50	3	3
MeOTf	**4a**	KOH	10	−15	DMF	60	34	5	3
MeOTf	**4a**	KOH	2	−15	DMF	7	76	3	3
MeOTf	**4a**	KOH	10	−15	CH_3CN	5	65	29	3
MeOTf	**4a**	KOH	10	−15	CH_3OH	0	100		3
MeOTf	**4a**	TBAH	6	−15	DMF	5	77	9	3
MeOTf	**4a**	TBK	saturated	−15	DMF	40	3	56	3
MeI	**4a**	KOH	10	80	DMF	57 ± 5	36 ± 3	3 ± 3	6
MeI	**4a**	TBAH	4	80	DMF	83 ± 4	13 ± 3	2 ± 1	9
MeI	**4a**	TBAH	2	80	DMF	84 ± 1	11 ± 1	4 ± 1	4
MeI	**5a**	TBAH	2	80	DMF	84 ± 1	11 ± 1	4 ± 1	4
MeI	**6a**	TBAH	2	80	DMF	84 ± 1	11 ± 1	4 ± 1	4

[a] Reaction times for the reaction with [^{11}C]methyl triflate and [^{11}C]methyl iodide were 3 and 4 min, respectively, for 1 mg of desmethyl precursor **4a**, **5a** and **6a**. Data points with $n > 3$ represent the mean ± SD. HMPA= hexamethylphosphoramide; TBAH = tetrabutylammonium hydroxide; TBK= potassium *tert*-butoxide.

Table 2. Tissue Biodistribution of [^{11}C]**4** in Albino Male CD Rats[a]

tissue	5 min	15 min	30 min	60 min	90 min
blood	0.20 ± 0.05	0.09 ± 0.05	0.06 ± 0.02	0.06 ± 0.02	0.04 ± 0.01
plasma	0.16 ± 0.04	0.09 ± 0.04	0.06 ± 0.02	0.05 ± 0.01	0.05 ± 0.01
heart	1.79 ± 1.03	2.62 ± 1.87	2.58 ± 1.35	2.09 ± 0.83	2.38 ± 0.82
lung	4.00 ± 1.74	3.32 ± 2.08	2.00 ± 0.83	1.48 ± 0.15	1.21 ± 0.18
liver	0.37 ± 0.19	0.59 ± 0.30	0.43 ± 0.12	0.41 ± 0.03	0.40 ± 0.08
adrenal gland	0.77 ± 0.55	2.29 ± 1.90	2.99 ± 2.71	4.00 ± 1.69	3.74 ± 0.74
kidney	0.79 ± 0.30	1.17 ± 0.74	1.05 ± 0.45	1.14 ± 0.23	1.34 ± 0.32
spleen	0.28 ± 0.22	1.27 ± 0.88	1.46 ± 0.61	1.55 ± 0.19	1.56 ± 0.44
testicle	0.06 ± 0.03	0.12 ± 0.09	0.13 ± 0.07	0.15 ± 0.06	0.20 ± 0.05
intestine	0.30 ± 0.17	0.78 ± 0.54	0.55 ± 0.27	0.62 ± 0.18	0.68 ± 0.15
muscle	0.19 ± 0.11	0.25 ± 0.17	0.26 ± 0.14	0.14 ± 0.07	0.21 ± 0.10
pituitary	0.33 ± 0.09	0.49 ± 0.13	0.30 ± 0.07	0.36 ± 0.19	0.15 ± 0.06
cerebellum	0.25 ± 0.12	0.20 ± 0.12	0.12 ± 0.06	0.08 ± 0.00	0.09 ± 0.03
cortex	0.25 ± 0.14	0.17 ± 0.09	0.09 ± 0.04	0.06 ± 0.01	0.05 ± 0.01

[a] Radioactivity concentration is expressed as % of injected dose per gram of organ (%I.D./g). Values are expressed as mean ± SD. Data points for all tissues represent three rats, except for pituitary at 90 min = 2.

Analysis of authentic standards **5** and **6** and labeled radioligands [^{11}C]**5** and [^{11}C]**6** was carried out by liquid chromatography-APCI (LC-APCI) in order to confirm the identity of the two rotamers of each compound, which were previously characterized by NMR.[24] The LC-APCI chromatogram of **5** showed two main peaks (>95%) showing retention times at 10 and 11.30 min. Mass spectra of the two peaks both displayed an intense ion at *m*/*z* 333 corresponding to the protonated molecular ion (MH^+) of the two rotamers of **5**. Identity of [^{11}C]-**5** was ensured by its EI spectrum, which showed a base ion at *m*/*z* 86 ($C_5H_{12}N$) and ions at *m*/*z* 332 (MH^+), 275 ($M - C_4H_9$), 246 ($M - C_5H_{12}N$), and 218 ($M - C_6H_{12}NO$). The LC-APCI chromatogram of [^{11}C]**6** showed two main peaks at room temperature of 9.10 and 10 min. Mass spectra of these peaks both displayed an intense ion at *m*/*z* 351 corresponding to the protonaned molecular ion (MH^+) of the two rotamers of **6**.

The identity of the radioligands was also confirmed by HPLC. The authentic samples of **4**−**6** were co-injected with the labeled radioligands. The products coeluted with the standard (see Experimental Section).

Biodistribution Studies. The tissue biodistribution of [^{11}C]**4**, [^{11}C]**5**, and [^{11}C]**6** in vivo in albino male CD rats as a function of time is presented in Tables 2−4. Low radioligand uptake was observed within the brain, as previously observed for compound **1** of nonlesioned rats. Among the other tissues examined all radioligands exhibited a higher accumulation in organs known to be rich in PBR such as heart, lung, kidney, spleen, and particularly adrenal gland. In most of these organs the time of maximum radioligand accumulation was observed between 30 and 60 min after radioligand injection. The specificity of the in vivo binding of [^{11}C]**4**, [^{11}C]**5**, and [^{11}C]**6** to PBR was evaluated in separate groups of rats pretreated (5 mg/kg iv) with either compound **1** or vehicle immediately before radioligand injection. Results of inhibition experiments are presented in Table 5 and Figure 1. At 30 min after the injection of [^{11}C]**4**, [^{11}C]**5**, and [^{11}C]**6** a significant reduction of radioactivity concentration in the heart, lung, adrenal gland, kidney, and spleen but not in the blood of rats pretreated with compound **1** was observed. A significant reduction in radioactivity concentration was found also in the pituitary gland and cortex in animals injected with [^{11}C]**5** and [^{11}C]**6**, respectively.

Discussion

The aim of this study was to synthesize and evaluate the properties of [^{11}C]**4**, [^{11}C]**5**, and [^{11}C]**6** as potential radioligands to investigate PBRs in vivo. Since the compounds were never evaluated in animals, the first step of this project was focused to verify if [^{11}C]**4**, [^{11}C]-**5**, and [^{11}C]**6** distribute in normal rats according to the known regional expression of PBR in peripheral tissues.

The radioligands were efficiently synthesized by [^{11}C]-*N*-methylation from the corresponding desmethyl pre-

Table 3. Tissue Biodistribution of [^{11}C]**5** in Albino Male CD Rats[a]

tissue	5 min	15 min	30 min	60 min	90 min
blood	0.13 ± 0.01	0.08 ± 0.02	0.06 ± 0.01	0.03 ± 0.01	0.03 ± 0.01
plasma	0.12 ± 0.01	0.05 ± 0.01	0.03 ± 0.01	0.03 ± 0.00	0.02 ± 0.00
heart	0.86 ± 0.19	0.80 ± 0.19	1.21 ± 0.15	1.26 ± 0.19	1.23 ± 0.18
lung	3.09 ± 0.70	2.01 ± 0.42	2.34 ± 0.77	1.33 ± 0.25	1.27 ± 0.12
liver	0.64 ± 0.11	0.50 ± 0.14	0.55 ± 0.08	0.32 ± 0.04	0.27 ± 0.01
adrenal gland	1.32 ± 0.22	1.38 ± 0.32	2.54 ± 0.51	2.27 ± 1.03	1.80 ± 0.41
kidney	0.59 ± 0.17	0.60 ± 0.16	0.77 ± 0.25	0.78 ± 0.15	0.73 ± 0.09
spleen	0.50 ± 0.20	0.92 ± 0.17	1.25 ± 0.17	1.25 ± 0.29	1.06 ± 0.10
testicle	0.06 ± 0.01	0.05 ± 0.02	0.08 ± 0.01	0.09 ± 0.40	0.08 ± 0.00
intestine	0.25 ± 0.08	0.32 ± 0.09	0.40 ± 0.06	0.40 ± 0.07	0.37 ± 0.06
muscle	0.11 ± 0.03	0.14 ± 0.09	0.16 ± 0.02	0.12 ± 0.03	0.12 ± 0.01
pituitary	0.22 ± 0.05	0.20 ± 0.07	0.24 ± 0.09	0.25 ± 0.06	0.20 ± 0.02
cerebellum	0.13 ± 0.03	0.08 ± 0.02	0.09 ± 0.01	0.05 ± 0.01	0.04 ± 0.00
cortex	0.12 ± 0.03	0.07 ± 0.02	0.07 ± 0.02	0.04 ± 0.01	0.03 ± 0.00

[a] Radioactivity concentration is expressed as % of injected dose per gram of organ (%I.D./g). Values are expressed as mean ± SD. Data points for all tissues represent three rats.

Table 4. Tissue Biodistribution of [^{11}C]**6** in Albino Male CD Rats[a]

tissues	5 min	15 min	30 min	60 min	90 min
blood	0.11 ± 0.07	0.14 ± 0.03	0.11 ± 0.04	0.08 ± 0.02	0.05 ± 0.02
plasma	0.11 ± 0.07	0.09 ± 0.03	0.06 ± 0.01	0.06 ± 0.04	0.04 ± 0.01
heart	0.68 ± 0.49	0.86 ± 0.21	0.73 ± 0.23	0.60 ± 0.25	0.58 ± 0.11
lung	2.37 ± 2.41	2.25 ± 0.54	2.09 ± 1.00	1.77 ± 1.05	1.55 ± 0.41
liver	0.41 ± 0.29	0.69 ± 0.10	0.55 ± 0.10	0.45 ± 0.11	0.39 ± 0.09
adrenal gland	1.12 ± 0.91	2.53 ± 0.47	2.78 ± 0.37	2.85 ± 0.36	2.22 ± 0.54
kidney	0.41 ± 0.30	0.73 ± 0.08	0.55 ± 0.13	0.51 ± 0.23	0.46 ± 0.11
spleen	0.34 ± 0.24	0.75 ± 0.10	0.77 ± 0.30	0.65 ± 0.29	0.71 ± 0.13
testicle	0.04 ± 0.03	0.09 ± 0.02	0.09 ± 0.02	0.09 ± 0.09	0.08 ± 0.01
intestine	0.18 ± 0.13	0.37 ± 0.12	0.31 ± 0.07	0.25 ± 0.09	0.24 ± 0.05
muscle	0.06 ± 0.06	0.13 ± 0.00	0.10 ± 0.05	0.07 ± 0.04	0.08 ± 0.02
pituitary	0.16 ± 0.11	0.27 ± 0.14	0.12 ± 0.03	0.14 ± 0.04	0.15 ± 0.02
cerebellum	0.10 ± 0.07	0.11 ± 0.02	0.09 ± 0.03	0.07 ± 0.02	0.06 ± 0.01
cortex	0.10 ± 0.07	0.11 ± 0.02	0.1 ± 0.03	0.07 ± 0.02	0.06 ± 0.01

[a] Radioactivity concentration is expressed as % of injected dose per gram of organ (%I.D./g). Values are expressed as mean ± SD. Data points for all tissues represent three rats.

Table 5. Tissue Concentration of Radioactivity at 30 min Post-Injection of [^{11}C]**4**, [^{11}C]**5**, and [^{11}C]**6** into Albino Male CD Rats[a] After Pretreatment with Cold PK 11195 or Vehicle

	[^{11}C]**4**			[^{11}C]**5**			[^{11}C]**6**		
tissue	vehicle	PK 11195-pretreated	*p*	vehicle	PK 11195-pretreated	*p*	vehicle	PK 11195-pretreated	*p*
blood	0.01 ± 0.01	0.02 ± 0.003	NS	0.03 ± 0.01	0.06 ± 0.01	*	0.04 ± 0.01	0.04 ± 0.01	NS
heart	0.35 ± 0.04	0.04 ± 0.01	*	0.77 ± 0.07	0.13 ± 0.08	**	0.35 ± 0.03	0.11 ± 0.01	**
lung	0.35 ± 0.22	0.05 ± 0.01	*	0.91 ± 0.39	0.14 ± 0.04	*	0.56 ± 0.30	0.12 ± 0.01	*
liver	0.08 ± 0.04	0.16 ± 0.06	*	0.30 ± 0.06	0.56 ± 0.09	*	0.35 ± 0.03	0.45 ± 0.07	*
adrenal gland	0.62 ± 0.62	0.17 ± 0.02	*	1.60 ± 0.16	0.94 ± 0.85	NS	1.79 ± 0.61	0.78 ± 0.12	**
kidney	0.19 ± 0.12	0.05 ± 0.02	*	0.45 ± 0.02	0.16 ± 0.06	*	0.35 ± 0.26	0.12 ± 0.01	NS
spleen	0.26 ± 0.16	0.02 ± 0.01	*	0.56 ± 0.16	0.11 ± 0.06	*	0.28 ± 0.02	0.09 ± 0.01	**
muscle	0.03 ± 0.02	0.02 ± 0.01	NS	0.09 ± 0.01	0.07 ± 0.06	NS	0.05 ± 0.01	0.03 ± 0.01	**
pituitary	0.11 ± 0.07	0.09 ± 0.06	NS	0.25 ± 0.1	0.07 ± 0.05	*	0.09 ± 0.03	0.06 ± 0.04	NS
cortex	0.02 ± 0.01	0.02 ± 0.01	NS	0.05 ± 0.01	0.04 ± 0.02	NS	0.05 ± 0.0048	0.02 ± 0.003	**

[a] Radioactivity concentration is expressed as % of injected dose per gram of organ (%I.D./g). Values are expressed as mean± SD of five rats. Differences between groups were examined with Student *t*-test. NS = not significant ($p > 0.05$); *significant ($p \leq 0.05$); **very significant ($p \leq 0.001$).

cursors in high yields and high specific radioactivity to perform animal studies. The radioligands are rapidly taken up and retained in tissues rich in PBR such as heart, adrenal gland, kidney, and spleen. In lungs, where PBRs are also expressed, we observed a high initial accumulation of the radioligands (4% for [^{11}C]**4**, 3% for [^{11}C]**5**, and 2.4% for [^{11}C]**6** I.D./g of tissue, respectively) followed by a continuous decrease. Between the various organs examined the highest accumulation of radioactivity was found in the adrenal gland, the organ with the higher concentration of PBR.[8] In this tissue at 30 min after injection approximately the %I.D./g of tissue was 3.0%, 2.2%, and 2.8% for [^{11}C]-**4**, [^{11}C]**5**, and [^{11}C]**6**, respectively. At this time radioligand [^{11}C]**4** displayed the highest tissue-to-blood radioactivity concentration (50) in comparison with [^{11}C]**5** (42) or [^{11}C]**6** (25), respectively. In the kidney the behavior of [^{11}C]**4** and [^{11}C]**5** was similar whereas a lower signal-to-noise ratio was observed for [^{11}C]**6**. Also in the heart higher radioactivity concentration as well as tissue-to-lung radioactivity ratios were observed in the group of rats injected with compound [^{11}C]**4**. Heart-to-lung radioactivity ratios progressively increased with time in rats treated with either [^{11}C]**4** or [^{11}C]**5**; however, only in the case of [^{11}C]**4** did they reach values higher than 1.

Results of inhibition studies in peripheral tissues suggest that radioligand uptake in heart, lung, adrenal gland, kidney, and spleen was due to specific binding of the radioligands with PBR (Table 5). In these organs

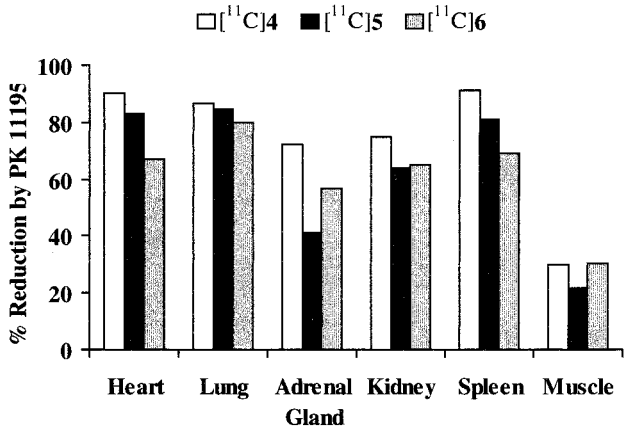

Figure 1. Effect of pretreatment with PK 11195 on radioactivity concentration in tissues 30 min after injection of [^{11}C]-**4**, [^{11}C]**5**, or [^{11}C]**6**. Data are presented as a percentage of reduction of radioligand radioactivity concentration in rats treated with 5 mg/kg PK 11195 compared to vehicle-treated rats.

approximately 70−90% of [^{11}C]**4** uptake and 60−90% of [^{11}C]**5** and [^{11}C]**6** uptake was inhibited by the preadministration of 5 mg/kg of **1**. A significant reduction (70%) was also observed in the pituitary gland of the group of rats injected with [^{11}C]**5** but not in the group of rats treated with either [^{11}C]**4** or [^{11}C]**6**.

The relatively low specific binding obtained in the inhibition experiments in the adrenal gland with radioligands [^{11}C]**5** (41%) and [^{11}C]**6** (56%) compared with [^{11}C]**4** (72%) was expected based on the racemic nature of **5** and **6**. The enantiomers may behave differently in vivo with respect to specific receptor binding.[33,34] Thus, the presence of an inactive isomer might increase only the amount of unspecific binding and consequently reduce the signal-to-noise ratio. However, if the (*R*)- or (*S*)-isomers of **5** and **6** differ on PBRs requires further investigation.

Pretreatment with compound **1** increased liver uptake in animals injected with either [^{11}C]**4**, [^{11}C]**5**, or [^{11}C]**6**. A similar increase of radioactivity concentration was observed in the liver of mice injected with [^{3}H]**1** plus 5 mg/kg of cold compound.[35]

The uniform distribution of the radiolabeled compounds [^{11}C]**4**, [^{11}C]**5**, and [^{11}C]**6** within the rat brain was in agreement with the low expression of PBR in the brain of nonlesioned rats. At 60 min after injection of the radioligands the highest stable uptake was found in the pituitary (0.36% for [^{11}C]**4**, 0.25% for [^{11}C]**5**, and 0.14% for [^{11}C]**6**, respectively) compared to that found in the other areas such as cerebellum and cortex (Figure 2).

In conclusion, results of this study indicate that [^{11}C]-**4**, [^{11}C]**5**, and [^{11}C]**6** are promising radioligands for the in vivo imaging of PBR. Among these, radioligand [^{11}C]-**4** showed a higher specific binding to PBR as indicated by the high reduction of radioligand uptake observed in the inhibition study with cold PK 11195 and tissue-to-blood ratio. Due to its easy preparation and in vivo behavior [^{11}C]**4** seems to be a suitable radioligand for the quantification and visualization of PRBs with PET. Further studies in appropriate animal models of brain injuries or inflammation should confirm the potential interest of [^{11}C]**4** for the in vivo imaging of PBR.

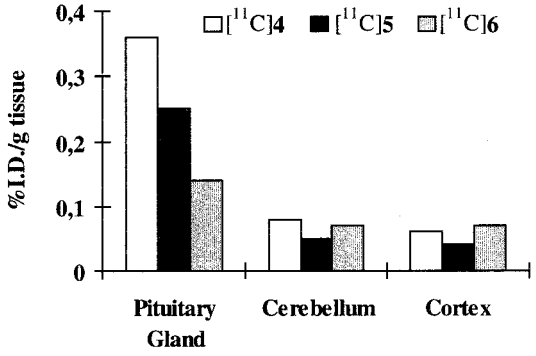

Figure 2. Radioactivity distribution in rat brain measured 60 min after injection of [^{11}C]**4**, [^{11}C]**5**, or [^{11}C]**6**. Data are presented as the mean value of radioactivity concentration in the pituitary gland, cerebellum, and cortex ($n = 3$).

Experimental Section

Materials. Reagents and solvents were obtained from Aldrich Italia S.p.A. (Milano, Italy) and were HPLC or American Chemical Society (ACS) grade.

[^{11}C]Carbon dioxide was produced by the ^{14}N(p,α)^{11}C reaction on a CTI-Siemens RDS-112 cyclotron, using 11.5 MeV proton beam at currents 10−30 μA, and trapped in a hollow stainless steel loop, cooled with liquid nitrogen. [^{11}C]Methyl iodide was synthesized as described by Långström[36] involving the reduction of [^{11}C]CO_2 with $LiAlH_4$ to lithium aluminum [^{11}C]methylate, hydrolysis of this intermediate organometallic complex, and subsequent iodination of the formed [^{11}C]methanol with hydriodic acid and distillation through an Ascarite-Sicapent purification column. [^{11}C]Methyl triflate was prepared as described by Jewett[37] from [^{11}C]methyl iodide on silver triflate-graphitized column. Radiochemical syntheses were performed on the fully automated synthesis module (PET tracer synthesizer, Nuclear Interface Datentechnik GmbH, Münster, Germany) for [^{11}C]methylation.

The EI spectra were obtained with sample introduction into a particle beam HP 5988 instrument operating at 70 eV. The instrument was acquiring data from *m/z* 50 to *m/z* 500. The LC-APCI analyses were carried out with a Finnigan MAT95 double-focusing mass spectrometer. The corona discharge was set at 2 μA, the vaporizer at 350 °C, and the heated capillary at 200 °C. Chromatographic separation of the two rotamers of [^{11}C]**5** and [^{11}C]**6** was achieved using a Hypersil-BDS C-18 (250 × 4.6 mm; 5 μm) reverse-phase column at 1 mL/min with a solvent mixture of H_2O:CH_3CN (40:60, v:v). The HPLC column end was connected to the APCI source. Purified samples were introduced directly into the APCI source by loop injection technique using H_2O:CH_3OH (1:1) at 0.3 mL/min by a Rheodyne injector with a 20-μL loop. Acquisition was carried out in Lcent mode scanning over the 100−900 mass range.

The course of the [^{11}C]methylations was assessed by radio-HPLC using CH_3CN−25 mM sodium dihydrogen orthophosphate as eluent at 1 mL/min. HPLC was performed with a Waters Millennium system equipped with UV absorbance detector set at 254 nm, a flow radioactivity detector (Bioscan), and a reversed-phase analytical HPLC column (Shandon Hypersil BDS C-18, 5 μm, 250 × 4.6 mm). pH of the final solutions was measured on a Schott Geräte pH meter.

Sterility and pyrogenity tests were performed according to Italian Pharmacopoeia[38] and using the Limulus Amebocyte Lysate (LAL) test (Bio Whittaker, Inc.), respectively.

Procedures for the Radiosyntheses of [^{11}C]4, [^{11}C]5, and [^{11}C]6. The radiosyntheses of [^{11}C]**4b**, [^{11}C]**5b** and [^{11}C]-**6b** were accomplished by reaction of [^{11}C]methyl iodide or [^{11}C]-methyl triflate with the corresponding desmethyl precursors in the presence of a base such as potassium hydroxide or tetrabutylammonium hydroxide (Scheme 1).

No-Carrier-Added Radiosyntheses. In the experiments addressed to the setting of optimal synthetic conditions (temperatures, solvent, [^{11}C]synthone and base) radioactivity was measured in an ascarite/molecular sieves activated carbon

Scheme 1. Radiolabeling of the New Quinoline-2-carboxamide Analogues of PK 11195

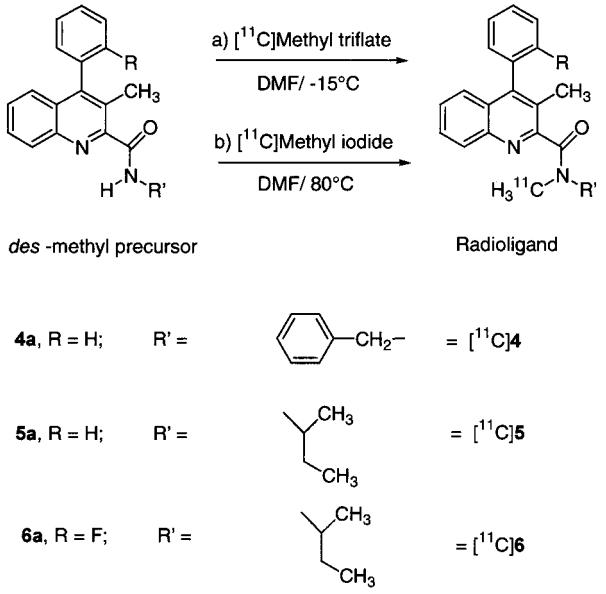

trap placed at the reactor outlet. The reaction mixture was then analyzed by HPLC ant the percent distribution of radioactivity among the [^{11}C]methylated target compound, [^{11}C]methanol, and other radioactive impurities was determined on the basis of the radioactivity peak.

(a) Methylation with [^{11}C]Methyl Triflate. In a closed reaction vial containing 1 mg of desmethyl precursor **4a** (0.0028 mmol) or **5a** (0.0031 mmol) or **6a** (0.003 mmol) and 10 μL (10 μmol) of 1 N potassium hydroxide in dimethylformamide (100 μL) [^{11}C]methyl triflate was transported by a stream of argon (10 mL/min) at −15 °C. At the end of trapping (3 min) the reaction mixture was diluted with 0.8 mL of mobile phase prior to injection into the HPLC semipreparative reversed-phase column (see below).

(b) Methylation with [^{11}C]Methyl Iodide. [^{11}C]Methyl iodide was transported by a stream of argon (5 mL/min) into the reaction vessel containing 1 mg of desmethyl precursor **4a** (0.0028 mmol) or **5a** (0.0031 mmol) or **6a** (0.003 mmol) in of 100 μL of dimethylformamide containing 1 μL (2 μmol) of tetrabutylammonium hydroxide (60% aqueous solution; Fluka) at 80 °C. After 4 min the reaction mixture was diluted with 0.8 mL of a solution of acetonitrile:water (1:1; v:v) and injected into the HPLC semipreparative reversed-phase column. Purification of each radioligand was accomplished using an HPLC Shandon Hypersil BDS C-18 (250 × 10 mm, 5 μm) column using the following chromatographic conditions: (1) [^{11}C]**4**: CH_3CN:5 mM sodium dihydrogen orthophosphate (65:35, v:v) at 4 mL/min flow rate (retention times were 8.5 and 11.5 min for [^{11}C]**4** and **4a**, respectively); (2) [^{11}C]**5** and [^{11}C]**6:** CH_3CN:5 mM sodium dihydrogen orthophosphate (60:40, v:v) at 4 mL/min flow rate (retention times were 9.2−11.2 min for the [^{11}C]-**5** rotamers and 12.5 min for **5a**, respectively, and 8.4−9.5 min for the [^{11}C]**6** rotamers and 11 min for **6a**, respectively).

Retention times were confirmed before each radiosynthesis by comparison with authentic standards. The effluent from the column corresponding to [^{11}C]**4**, [^{11}C]**5** or [^{11}C]**6** was collected in 40 mL of sterile water, and the radioligand was recovered by solid-phase extraction on Sep-Pak C-18 cartridge (Millipore) preactivated with 5 mL of MeOH followed by 10 mL of water. The Sep-Pak was washed with water (10 mL) before eluting with ethanol (0.5 mL) in a vial containing 5 mL of saline solution, which was sterilized through a sterile 0.22-μm filter (Gelman Acrodisc). The pH of the final solution was ranging from 6.5 to 7.

The final solution of known volume of each radioligand was assayed for total radioactivity and a 20-μL aliquot was applied to an analytical HPLC Shandon Hypersil BDS C-18 (250 × 4.6 mm, 5 μm) column. The amount of carrier was calculated from the UV absorbance peak area by means of the external standard calibration plot. Chromatographic conditions used for each radioligand were CH_3CN:25 mM sodium dihydrogen orthophosphate (75:25, v:v) at 1 mL/min flow rate. Retention times were 6 and 7.1 min for [^{11}C]**4** and **4a**, respectively; 5.5−6.1 min for the two rotamers of [^{11}C]**5** and 6.8 min for the precursor **5a**, respectively; 5.2−5.6 min for the two rotamers of [^{11}C]**6** and 6.5 min for the precursor **6a**, respectively). The minimal detectable concentration was 0.51 nmol/mL for [^{11}C]-**4**, 2.2 nmol/mL for [^{11}C]**5**, and 2.2 nmol/mL for [^{11}C]**6**.

Carried-Added Radiosyntheses of [^{11}C]4, [^{11}C]5, and [^{11}C]6. The synthesis was carried out as described above for the no-carried-added preparation but 20 μL of methanol carrier was added to the hydriodic acid used for [^{11}C]methyl iodide formation. After semipreparative HPLC purification the fraction corresponding to the desired radioligand was collected in 40 mL of sterile water and the product was recovered by solid-phase extraction on a preactivated Sep-Pak C-18 cartridge by elution with 1 mL of methanol. The nonradioactive material with the ^{11}C-labeled radioligands was ensured by the well-detectable UV peak at the retention time of the target compound. The peak was collected and its identity was confirmed by mass spectrometry. Addition of authentic standard to the preparation before HPLC analysis caused the expected increase of the UV peak coeluting with the radioactive material.

In Vivo Studies with [^{11}C]4, [^{11}C]5, and [^{11}C]6. Tissue Distribution Studies. Biodistribution studies in rats were performed in conformity with the demands of the Laboratory Animal Ethical Committee (IACUC) of the Scientific Institute H San Raffaele, Milano, Italy. Albino male CD rats weighing 225−250 g were obtained from Charles River (Italy) which were injected in the tail vein with [^{11}C]**4**, [^{11}C]**5**, or [^{11}C]**6** as follows: (1) [^{11}C]**4**: injected dose of 100−150 μCi/100−150 μL of saline/animal (2 ± 1 Ci/μmol of specific radioactivity at time of injection); (2) [^{11}C]**5**: injected dose of 180−200 μCi/120−150 μL of saline/animal (1 ± 0.04 Ci/μmol of specific radioactivity at time of injection); (3) [^{11}C]**6**: injected dose of 150−200 μCi/150−180 μL of saline/animal (1 ± 0.1 Ci/μmol of specific radioactivity at time of injection).

At 5, 15, 30, 60 and 90 min, rats (three animals at each time point) were sacrificed by decapitation under slight ether anaesthesia and blood was collected into a heparinized tube. Plasma was separated by centrifugation and both blood and plasma were counted. Immediately after killing, the brain was removed quickly and dissected into cerebellum, whole cortex and pituitary gland. Peripheral organs, including heart, lung, liver, kidney, adrenal gland, spleen, testicle, intestine and muscle, were sampled and washed with cold saline. Tissue samples were then placed in preweighed tubes and assayed for the radioactivity by an automated well counter (LKB Compugamma CS 1282). In particular were sampled the whole kidney, adrenal gland, spleen, testicle, and heart, the duodenum, and the right deltoid muscle. One piece of the left, right and median lobes of the liver or one piece of anterior, median and posterior right lobes of the lungs were considered representative of the whole organ, i.e., liver or lung, placed in the same tube and counted. After counting samples were weighed and the uptake of radioactivity was calculated as a percentage of the injected dose per gram of tissue (%I.D./g tissue).

Inhibition Studies. Inhibition studies were performed in separate groups of rats. Animals (five rats each group) were injected in a tail vein with either 30 μL of **1** dissolved in DMSO: EtOH solution (1:1; v:v) or vehicle prior to the administration of the radioligands: (1) 1.4 mg (0.0039 mmol) of **1** followed by injection of 90−100 μCi of [^{11}C]**4**/130−150 μL of saline/animal (0.9 Ci/μmol of specific radioactivity at time of injection); (2) 1.6 mg (0.0049 mmol) of **1** followed by injection of 100−120 μCi [^{11}C]**5**/130−150 μL of saline/animal (0.9 Ci/μmol of specific radioactivity at time of injection); (3) 1.4 mg (0.0039 mmol) of **1** followed by an injection dose of 140−170 μCi of [^{11}C]**6**/120−150 μL of saline/animal (1 Ci/μmol of specific radioactivity at time of injection).

At 30 min, animals were decapitated and processed as described above (%I.D./g of tissue). Differences between groups, i.e., PK 11195 versus saline-pretreated rats, were examined by Student's *t*-test for unpaired data. Differences were considered significant at P values lower than 0.05.

References

(1) Braestrup, C.; Squires, R. F. Specific Benzodiazepine Receptors in Rat Brain Characterized by High-Affinity [^{3}H]Diazepam Binding. *Proc. Natl. Acad. Sci. U.S.A.* **1977**, *74*, 3805−3809.

(2) Möhler, H.; Okada, T. Benzodiazepine Receptor: Demonstration in the Central Nervous System. *Science* **1977**, *198*, 849−851.

(3) DeLorey, T. M.; Olsen, R. W. γ-Aminobutyric Acid$_A$ Receptor Structure and Function. *J. Biol. Chem.* **1992**, *267*, 16747−16750.

(4) Langer, S. Z.; Arbilla, S. Limitations of the Benzodiazepine Receptor Nomenclature: a Proposal for a Pharmacological Classification as Omega Receptor Subtypes. *Fund. Clin. Pharmacol.* **1988**, *2*, 159−170.

(5) Verma, A.; Snyders, S. H. Peripheral Types Benzodiazepine Receptors. *Annu. Rev. Pharmacol. Toxicol.* **1989**, *29*, 307−322.

(6) Gavish, M.; Bachman, I.; Shoukrun, R.; Katz, Y.; Veenman, L.; Weisinger, G.; Weizman, A. Enigma of the Peripheral Benzodiazepine Receptor. *Pharmacol. Rev.* **1999**, *51*, 629−650.

(7) Bénavidès, J.; Malgouris, C.; Imbault, F.; Begasset, F.; Uzan, A.; Renault, C.; Dubroeucq, M.-C.; Guérémy, C.; Le Fur, G. Peripheral-Type Benzodiazepine Binding Sites in Rat Adrenals: Binding Studies with [^{3}H]PK 11195 and Autoradiographic Localization. *Arch. Int. Pharmacodyn. Ther.* **1983**, *266*, 38−49.

(8) De Souza, E. B.; Anholt, R. R. H.; Murphy, K. M. M.; Snyder, S. H.; Kuhar, M. J. Peripheral-Type Benzodiazepine Receptors in Endocrine Organs: Autoradiographic Localization in Rat Pituitary, Adrenal, and Testis. *Endocrinology* **1985**, *116*, 567−573.

(9) Anholt, R. R.; De Souza, E. B.; Oster-Granite, M. L.; Snyder, S. H. Peripheral-Type Benzodiazepine Receptors: Autoradiographic Localization in Whole-Body Sections of Neonatal Rats. *J. Pharmacol. Exp. Ther.* **1985**, *233*, 517−526.

(10) Bénavidès, J.; Quateronet, D.; Imbault, F.; Malgouris, C.; Uzan, A.; Renault, C.; Dubroeucq, M.-C.; Guérémy, C.; Le Fur, G. Labeling of "Peripheral-Type" Benzodiazepine Binding Sites in the Rat Brain Using [^{3}H]PK 11195, an Isoquinoline Carboxamide Derivative: Kinetic Studies and Autoradiographic Localisation. *J. Neurochem.* **1983**, *41*, 1744−1750.

(11) Anholt, R. R.; Pedersen, P. L.; De Souza, E. B.; Snyder, S. H. The Peripheral-Type Benzodiazepine Receptor. Localization to the Mitochondrial Outer Membrane. *J. Biol. Chem.* **1986**, *261*, 576−583.

(12) Diorio, D.; Welner, S. A.; Butterworth: R. F.; Meaney, M. J.; Suranyi-Cadotte, B. E. Peripheral Benzodiazepine Binding Sites in Alzheimer's Disease Frontal and Temporal Cortex. *Neurobiol. Aging* **1991**, *12*, 255−258.

(13) Bénavidès, J.; Cornu, P.; Dennis, T.; Dubois, A.; Hauw, J. J.; MacKenzie, E. T.; Sazdovitch, V.; Scatton, B. Imaging of Human Brain Lesions with an Omega3 Site Radioligand. *Ann. Neurol.* **1988**, *24*, 708−712.

(14) Vowinckel, E.; Reutens, D.; Becher, B.; Verge, G.; Evans, A.; Owens, T.; Antel, J. P. PK 11195 Binding to the Peripheral Benzodiazepine Receptor as a Marker of Microglia Activation in Multiple Sclerosis and Experimental Autoimmune Encephalomyelitis. *J. Neurosci. Res.* **1997**, *50*, 345−353.

(15) Schoemaker, H.; Morelli, M.; Deshmukh, P. [^{3}]Ro5-4864 Benzodiazepine Binding in the Kainate Lesioned Striatum and Huntington's Diseased Basal Ganglia. *Brain Res.* **1982**, *248*, 396−401.

(16) Banati, R. B.; Goerres, G. W.; Myers, R.; Gunn, R. N.; Turkheimer, F. E.; Kreutzberg, G. W.; Brooks, D. J.; Jones, T.; Duncan, J. S. [^{11}C](R)-PK 11195 positron emission tomography imaging of activated microglia in vivo in Rasmussen's encephalitis. *Neurology* **1999**, *53*, 2199−2203.

(17) Camsonne, R.; Crouzel, C.; Comar, D.; Mazière, M.; Prenant, C.; Sastre, J.; Moulin, M.; Syrota, A. Synthesis of N-[^{11}C]Methyl, N-(Methyl-1-Propyl), Chloro-2-Phenyl)-1 Isoquinoline Carboxamide-3 (PK-11195): a New Ligand for Peripheral Benzodiazepine Receptors. *J. Labeled Compds. Radiopharm.* **1984**, *21*, 985−991.

(18) Pike, V. W.; Halldin, C.; Crouzel, C.; Barrè, L.; Nutt, D. J.; Osman, S.; Shah, F.; Turton, D. R.; Waters, S. L. Radioligands for PET Studies of Central Benzodiazepine Receptors and PK (Peripheral Benzodiazepine) Binding Sites-Current Status. *Nucl. Med. Biol.* **1993**, *20*, 503−525.

(19) Junck, L.; Olson, J. M.; Ciliax, B. J.; Koeppe, R. A.; Watkins, G. L.; Jewett, D. M.; McKeever, P. E.; Wieland, D. M.; Kilbourn, M. R.; Starosta-Rubinstein, S.; Mancini, W. R.; Kuhl, D. E.; Greenberg, H. S.; Young, A. B. PET Imaging of Human Gliomas with Ligands For the Peripheral Benzodiazepine Binding Site. *Ann. Neurol.* **1989**, *26*, 752−758.

(20) Pappata, S.; Cornu, P.; Samson, Y.; Prenant, C.; Benavides, J.; Scatton, B.; Crouzel, C.; Hauw, J. J.; Syrota, A. PET Study of Carbon-11-PK 11195 Binding to Peripheral Type Benzodiazepine Sites in Glioblastoma: a Case Report. *J. Nucl. Med.* **1991**, *32*, 1608−1610.

(21) Junck, L.; Jewett, D. M.; Kilbourn, M. R.; Young, A. B.; Kuhl, D. E. PET Imaging of Cerebral Infarcts Using a Ligand for the Peripheral Benzodiazepine Binding Site. *Neurology* **1990**, *40*, 553P, 265.

(22) Charbonneau, P.; Syrota, A.; Crouzel, C.; Valois, J. M.; Prenant, C.; Crouzel, M. Peripheral-Type Benzodiazepine Receptors in the Living Heart Characterized by Positron Emission Tomography. *Circulation* **1986**, *73*, 476−483.

(23) Pascali, C.; Luthra, S. K.; Pike, V. W.; Price, G. W.; Ahier, R. G.; Hume, S. P.; Myers, R.; Manjil, L.; Cremer, J. E. The Radiosynthesis of [^{18}F]PK 14105 as an Alternative Radioligand for Peripheral Type Benzodiazepine Binding Sites. *Appl. Radiat. Isot.* **1990**, *41*, 477−482.

(24) Cappelli, A.; Anzini, M.; Vomero, S.; De Benedetti, P. G.; Menziani, M. C.; Giorgi, G.; Manzoni, C. Mapping the Peripheral Benzodiazepine Receptor Binding Site by Conformationally Restrained Derivatives of 1-(2-Chlorophenyl)-*N*-Methylpropyl)-3-Isoquinolinecarboxamide (PK 11195). *J. Med. Chem.* **1997**, *40*, 2910−2921.

(25) Shah, F.; Hume, S. P.; Pike, V. W.; Ashworth, S.; McDermott, J. Synthesis of the Enantiomers of [*N*-Methyl-^{11}C]PK 11195 and Comparison of their Behaviours as Radioligands for PK Binding Sites in Rats. *Nucl. Med. Biol.* **1994**, *21*, 573−581.

(26) Petit-Taboueˆ, M. C.; Baron, J. C.; Barrè, L.; Travère, J. M.; Speckel, D.; Camsonne, R.; MacKenzie, E. T. Brain Kinetics and Specific Binding of [^{11}C]PK 11195 to Omega3 Sites in Baboons: Positron Emission Tomography Study. *Eur. J. Pharmacol.* **1991**, *200*, 347−351.

(27) Skowronski, R.; Fanestil, D. D.; Beaumont, K. Photoaffinity Labeling of Peripheral-Type Benzodiazepine Receptors in Rat Kidney Mitochondria with [^{3}H]PK 14105. *Eur. J. Pharmacol.* **1988**, *148*, 187−193.

(28) Gildersleeve, D. L.; Van Dort, M. E.; Johnson, J. W.; Sherman, P. S.; Wieland, D. M. Synthesis and Evaluation of [^{123}I]-Iodo-PK11195 for Mapping Peripheral-Type Benzodiazepine Receptors (ω_3) in Heart. *Nucl. Med. Biol.* **1996**, *23*, 23−28.

(29) Gildersleeve, D. L.; Lin, T. Y.; Wieland, D. M.; Ciliax, B. J.; Olson, J. M.; Young, A. B. Synthesis of a High Specific Activity 125I-Labeled Analogue of PK 11195, Potential Agent for SPECT Imaging of the Peripheral Benzodiazepine Binding Site. *Int. J. Radiat. Appl. Instrum. B* **1989**, *16*, 423−429.

(30) Myers, R. Mitochondrial Benzodiazepine Receptor Ligands as Indicator of Damage in the CNS: their Application in Positron Emission Tomography. In *Peripheral Benzodiazepine Receptors*; Myers, R., Eds.; Academic Press: London, 1993; pp 235−273.

(31) Groom, G. N.; Junck, L.; Foster, N. L.; Frey, K. A.; Kuhl, D. E. PET of Peripheral Benzodiazepine Binding Sites in the Microgliosis of Alzheimer's Disease. *J. Nucl. Med.* **1995**, *36*, 2207−2210.

(32) Dumont, F.; De Vos, F.; Versijpt, J.; Jansen, H. M.; Korf, J.; Dierckx, R. A.; Slegers, G. In Vivo Evaluation in Mice and Metabolism in Blood of Human Volunteers of [^{123}I]Iodo-PK11195: a Possible Single-Photon Emission Tomography Tracer for Visualization of Inflammation. *Eur. J. Nucl. Med.* **1999**, *26*, 194−199.

(33) Simonyi, M.; Fitos, I.; Visy, J. Chirality of Bioactive Agents in Protein Binding Storage and Transport Process. *Trends Pharmacol. Sci.* **1986**, *7*, 112−116.

(34) Testa, B. Chiral Aspects of Drug Metabolism. *Trends Pharmacol. Sci.* **1986**, *7*, 60−64.

(35) Hashimoto, K.; Inoue, O.; Suzuki, K.; Yamasaki, T.; Kojima, M. Synthesis and Evaluation of 11C−PK 11195 for In Vivo Study of Peripheral-Type Benzodiazepine Receptors Using Positron Emission Tomography. *Ann. Nucl. Med.* **1989**, *3*, 63−71.

(36) Långström, B.; Lundqvist, H. The Preparation of [^{11}C]Methyl Iodide and its Use in the Synthesis of [^{11}C]Methyl-L-Methionine. *Int. J. Appl. Radiat. Isot.* **1976**, *27*, 357−363.

(37) Jewett, D. M. A Simple Synthesis of [^{11}C]Methyl Triflate. *Appl. Radiat. Isot.* **1992**, *43*, 1383−1385.

(38) *Italian Pharmacopoeia*; State Polygraphic Institute: Rome, 1985; pp 277−288.

JM001004H